One-step double autoionization into the double-photoionization continuum

R. Wehlitz,[1,*] M.-T. Huang,[1] K. A. Berrington,[2] S. Nakazaki,[3] and Y. Azuma[1]

[1]*Photon Factory, IMSS, KEK, Tsukuba, Ibaraki 305-0801, Japan*

[2]*School of Science and Mathematics, Sheffield Hallam University, Sheffield S1 1WB, United Kingdom*

[3]*Department of Materials Science, Faculty of Engineering, Miyazaki University, Miyazaki 889-2192, Japan*

(Received 24 November 1998)

We have determined the Fano parameters and oscillator strengths of the triply photoexcited Li $2s^2 2p\ ^2P^o$ autoionizing resonance in the Li^+ and Li^{2+} partial photoion yields. Using monochromatized photons we observed an asymmetric resonance profile not only in the Li^+ but also in the Li^{2+} partial cross section. The interaction between the triply excited state and the double-photoionization continuum takes place via a one-step double autoionization, since a two-step autoionization of the discrete state is energetically not possible. Our theoretical calculations using an *R*-matrix method for both the Li^+ and Li^{2+} partial cross sections show resonance profiles in good agreement with experimental result. [S1050-2947(99)50707-5]

PACS number(s): 32.80.Fb

For atomic photoexcitation resonances above the first ionization limit, autoionization becomes possible by the interaction with one or many single-photoionization continua. This leads to an asymmetric resonance profile and the production of singly charged ions [1,2]. A theoretical description of this process was introduced by Fano [3] and refined later by Shore [4] and Starace [5]. Above the second ionization limit, one-step double autoionization becomes possible by the interaction with the double-photoionization continua. Initial observations of such processes indicated symmetric profiles due to the small cross section for direct double photoionization [6,7]. The first indication of an asymmetric profile was observed in the case of sodium, albeit with low resolution [8]. These cases present a theoretical challenge, since the two ejected electrons will have a continuous distribution of energy sharing and calculations have to be made all over them. It should also be noted that in many cases doubly charged ions can be produced by two-step sequential single autoionization [7,9–11]. This is usually the much stronger channel when it is available, and the energy sharing will be limited to discrete values.

Lithium presents the purest case of electron correlation involving three electrons, with no other spectator electron. Photoprocesses directly involving all three electrons of the lithium atom came to be known through the discovery of triply photoexcited ''hollow lithium'' resonances [7,9,12–15], and the very recent measurement of direct triple photoionization of lithium [16]. One-step double autoionization in lithium is of strong interest because it involves processes that most directly measure the electron correlation involving three electrons in the excited state. The low-lying hollow lithium photoexcitation resonances below the doubly excited singly charged lithium-ion thresholds present cases where doubly charged ions can be produced only by one-step double autoionization, as can be seen in Fig. 1. Here we report the measurement of the resonance profiles and branching ratio for the singly and doubly charged ions for the lowest and well isolated $2s^2 2p\ ^2P^o$ ''*A*'' resonance.

The experiment was performed at the 2.5-GeV storage ring of the KEK Photon Factory. Photons coming from the undulator beam line BL16B were monochromatized by a 24-m spherical grating monochromator [17]. The monochromator's entrance and exit slits were set to 20 μm each. The position of the exit slit was optimized and a sufficiently high-photon-energy resolution of 39 meV was achieved.

The photon beam entered the experimental chamber, in-

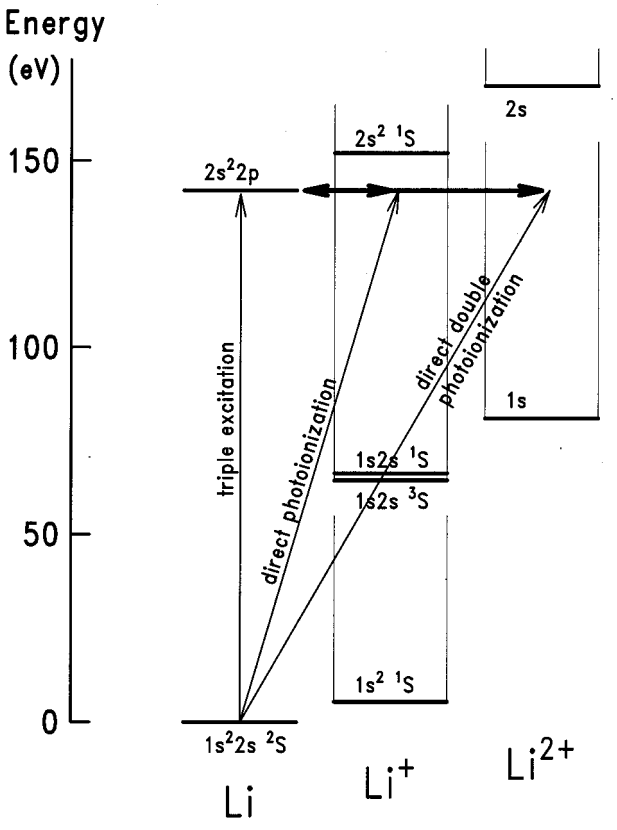

FIG. 1. Schematic energy-level diagram of ground-state Li. The relevant transitions are indicated by arrows. Note that the lowest autoionization resonance in the Li^+ channel ($2s^2\ ^1S$) is above the double-autoionizing resonance of interest.

*Electronic address: wehlitz@mail.kek.jp

tersecting a beam of Li atoms emerging from an effusive metal vapor oven [18]. The lithium photoions, which were produced in the interaction region, were detected with an ion time-of-flight spectrometer operating in the pulsed extraction mode, as described previously [7]. The background pressure in the experimental chamber during the experiment was lower than 1×10^{-7} mbar. The threshold of our constant-fraction discriminator (CFD) was set to a low level of 31 mV to ensure that there was no detection efficiency difference between the Li^+ and Li^{2+} ions; this was established experimentally by measuring the double-to-single photoionization ratio as a function of the CFD threshold.

In order to determine the line shapes and the corresponding Fano parameters of the $2s^22p(^2P)\rightarrow 1sn\ell+e^-$ and $2s^22p(^2P)\rightarrow 1s+2e^-$ transitions, we took several photon-energy scans from 141.5 to 143.5 eV with a step size of 6 meV. Partial ion-yield spectra were obtained in the gated time-of-flight (TOF) mode: Regions corresponding to the Li^+ and Li^{2+} charge states were defined in our ion-TOF spectrum, with additional regions to the left and right of both peaks included to record their corresponding background. Counts in these TOF regions were integrated and recorded simultaneously along with the relative photon flux for each photon energy. The relative photon flux was obtained from the drain current of the postfocusing mirror of the beam line. The relative photon flux was later put on an absolute scale using a calibrated photodiode [19]. After subtracting the appropriate background from the Li^+ and Li^{2+} signal, the intensity in each scan was normalized to the absolute photon flux. The resulting partial ion-yield spectra from each scan were added up and were scaled to the absolute photoabsorption cross-section data of Mehlman *et al.* [20], as shown in Fig. 2.

The partial ion-yield spectra exhibit the typical asymmetric Fano-shape profile not only for the Li^+ channel but also for the Li^{2+} channel. The asymmetric line shape of the $2s^22p$ resonance in the Li^{2+} channel, which was not observed earlier due to a lower energy resolution and inferior signal-to-noise ratio [7], demonstrates the coherent superposition of the direct double photoionization and the double-electron autoionization. However, since we do not detect the kinetic energy of the ejected electrons, we integrate over all possible kinetic energies of the electrons within their continuous energy distribution.

For a quantitative analysis we have applied the Fano formula [3] with an additional slowly varying, noninteracting background σ_b to our data

$$\sigma=\sigma_a\frac{(q+\epsilon)^2}{1+\epsilon^2}+\sigma_b\,, \tag{1}$$

with $\epsilon=2(E-E_0)/\Gamma$. Here, q is the profile index, which depends on the relative strength of the dipole transitions and Coulomb transition, E is the excitation energy, E_0 is the energy position of the resonance, and Γ the resonance width. σ_a represents the part of the continuum cross section that interacts with the discrete level. The parameter ρ is defined as

$$\rho^2=\frac{\sigma_a}{\sigma_a+\sigma_b}, \tag{2}$$

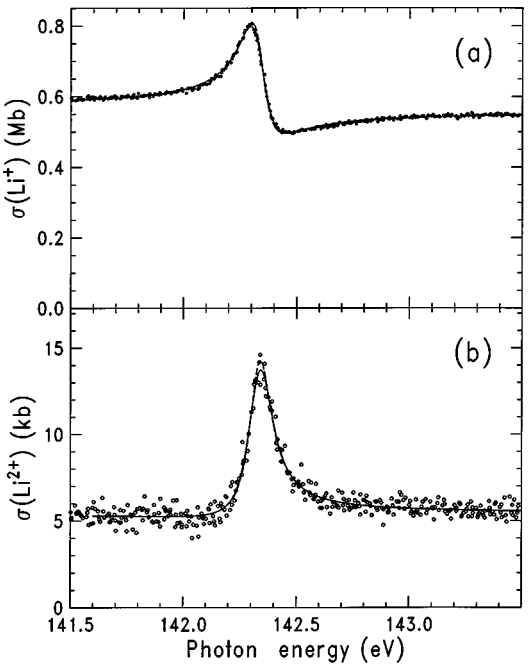

FIG. 2. Line profile of the Li $2s^22p\ ^2P^o$ resonance autoionizing into (a) the Li^+ channel and (b) the Li^{2+} channel. The solid line is a least-squares fit to our data and the dashed line is the same curve deconvoluted with the monochromator's bandpass. Note that the deconvoluted curve is barely visible at its maximum.

which measures the relative strength of the interaction using σ_a and σ_b as defined above. In order to fit a Fano profile to our data Eq. (1) was convoluted with a triangular instrument function of 39-meV full width at half maximum in a procedure that was used previously [7]. The Fano parameters obtained are presented in Table I and compared with previous results where possible. The absolute energy position of the resonance in the Li^+ channel was adjusted to a value of $E_0=142.33$ eV, as measured previously [7]. The resonance position in the Li^{2+} channel, as determined by the least-squares fit, is the same to within 0.004 eV. The width Γ is expected to be the same for both decay channels; nevertheless, since we have two independent ion-yield spectra, we obtain two values for Γ, which are the same within their error bars. There is good agreement with previous measurements of the width of the resonance, but the absolute value of q is generally smaller, except for the experimental q value for photoabsorption in [14].

A large profile index q close to infinity results in a symmetric (Lorentzian) line profile indicating no interaction, while $q=0$ would indicate a very strong interaction between the ionization channels. The fact that the profile index q for the Li^{2+} partial ion-yield is neither very large nor zero shows that there is a small interaction between the direct double-photoionization continuum and the triply excited $2s^22p\ ^2P^o$ state, giving rise to an interference that manifests itself in an asymmetric Fano profile. It is worthwhile to mention that the nonresonant double-to-single photoionization ratio at the resonance position is 1.0(1)%, in good agreement with previous measurements [7,22]. The oscillator strength of this resonance can be calculated from the resonance parameters [23]. From the oscillator strengths, given in Table I, one

TABLE I. Comparison of the Li $2s^2 2p\ ^2P^o$ resonance parameters. The width Γ is given for the total ionization cross section. f^+ and f^{2+} are the oscillator strengths for the Li^+ and Li^{2+} channel, respectively.

Reference	Γ (eV)	$q(Li^+)$	$q(Li^{2+})$	f^+	f^{2+}
Experiment	0.124(3)	−1.87(3)	6.9(7)	2.2×10^{-3}	7.3×10^{-5}
Theory	0.123	−2.17	3.13		
[12] (expt.)	0.20(4)	−2.2(6)[a]			
[13] (expt.)	0.14(2)	−2.0(3)			
[7] (expt.)	0.15(2)	−2.0(5)	∞		
[21] (theor.)	0.117				
[14] (expt.)	0.20(4)	−1.4(4)[a]			
[14] (theor.)	0.132	−1.86[a]			
[15] (expt.)	0.118(3)				
[15] (theor.)	0.13				
[24] (theor.)	0.123				

[a]The profile index q is given only for the total ionization cross section.

obtains an oscillator-strength ratio $f^{2+}/f^+ = 3.4\%$ demonstrating the greatly enhanced production of Li^{2+} ions.

In the Berrington and Nakazaki [24] calculation, use was made of a unified approach to direct and indirect ionization processes (double photoionization and double autoionization) within an R-matrix formulation [25]: representing the three-electron initial state ($^2S^e$) and final state ($^2P^o$) by a close-coupling expansion in the same two-electron core states. For the final state, this included the following channels: $1s^2kp$, $1s2\ell k\ell$, $1s3\ell k\ell$, $1s\overline{1\ell}k'\ell'$, and $2\ell 2\ell' \underline{k'}\ell''$, where the $k\ell$ represent a continuum electron and $1s\overline{1\ell}$ are pseudostates approximating the double continuum. The latter are defined in Berrington and Nakazaki, and we will return to this point later. We employ a method [the Quigley-Berrington (QB) method [26]] utilizing analytic properties of R-matrix theory to analyze resonance structures. The double-photoionization cross section is obtained in the calculation by summing the continuum pseudostate cross sections, which contain both resonant and nonresonant interactions.

Figure 3 shows the calculated resonance profiles with energies offset by 5.65 eV to higher energies. An energy shift of 5.39 eV, which corresponds to the binding energy of the $2s$ electron, is necessary because the calculation in the unified approach was performed using the incident energy of electron-impact excitation of Li^+ to obtain the cross sections for both the $e^- + Li^+$ excitation *and* $\gamma + Li$ process. An additional shift of 0.26 eV was introduced to match the calculated curves with the experimental data. Figure 3(a) shows the theoretical calculation along with the experimental data for the Li^+-ion yield. Our data were normalized using absolute cross-section measurements of Mehlman *et al.* [20], which are reported to have a systematic error bar of 20%. Although our calculated curve is on a slightly different cross-section scale than the experimental data, both data sets are in excellent agreement, taking this error into account.

In Fig. 3(b) we compare the theoretical calculation with the experimental data for the Li^{2+}-ion yield. The asymmetry of the resonance is reproduced fairly well and the sign of the q value, which is opposite the one for the Li^+-ion yield, is predicted correctly (see Table I). However, the size of the resonance as well as the nonresonant double-ionization cross section are overestimated. The calculated nonresonant double-to-single ionization ratio is about 2%.

A possible explanation for this disagreement is that the pseudostate basis used in the calculation here may not be fully optimum for direct double photoionization. However, the calculation in Ref. [24] using the same pseudostates gave good agreement with experiment for the electron-impact ionization cross section. While this process involves *many* partial waves, the direct double photoionization, although leading to the same final state ($Li^{2+} + 2e^-$), involves only *one* partial wave ($^2P^o$). Nevertheless, the interference between direct and indirect processes seems to be well represented.

In summary, we have measured the asymmetric line pro-

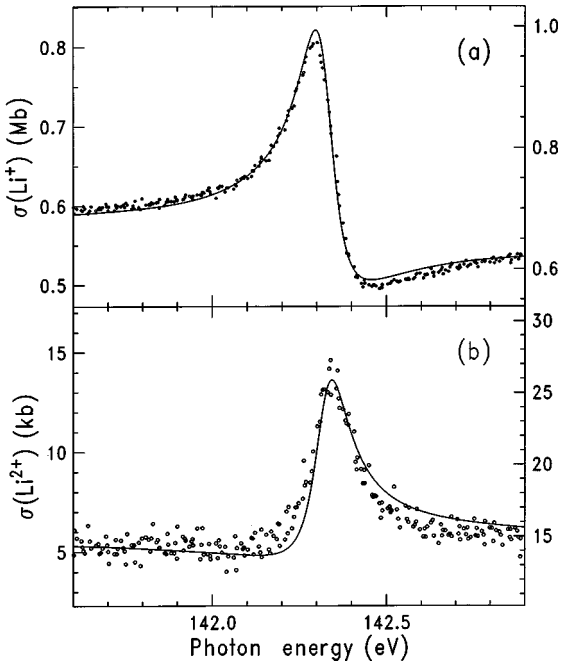

FIG. 3. Comparison of our experimental results for photoexcitation (open circles) with our photoexcitation calculations (solid lines). (a) Li^+ partial photoionization cross section; (b) Li^{2+} partial photoionization cross section. The scale on the left side is for the experimental data and the scale on the right side is for the theoretical curves.

files in the partial ion-yield spectra of Li^+ and Li^{2+} with high-energy resolution after resonant photoexcitation from the ground state of Li to the $2s^2 2p\ ^2P^o$ triply excited state. Since a two-step decay of this triply excited state into the double-photoionization continuum is energetically not possible, the asymmetric line profile clearly demonstrates an interaction between the direct double-photoionization process and the double-electron autoionization process, in which both electrons are emitted simultaneously. The measurement of the resonance profile in coincidence with double-autoionizing electrons of selected kinetic energies is expected to be difficult, but may be a very interesting future experiment.

Our R-matrix calculations confirm the asymmetric shape of the resonance profiles for single and double ionization. In particular, the q parameter and the change of its sign are very similar in the experimental photoionization spectra and the theoretical photon-scattering calculations.

We thank the Japanese Ministry of Education, Culture, and Science (Monbusho) and the Matsuo Foundation for financial support. R.W. gratefully acknowledges financial support from the Japan Society for the Promotion of Science. This work was performed with the approval of the Photon Factory Program Advisory Committee (Proposal No. 96G137).

[1] R. P. Madden and K. Codling, Phys. Rev. Lett. **10**, 516 (1963).
[2] K. Codling, R. P. Madden, and D. L. Ederer, Phys. Rev. **155**, 26 (1967).
[3] U. Fano, Phys. Rev. **124**, 1866 (1961).
[4] B. W. Shore, Phys. Rev. **171**, 43 (1968).
[5] A. F. Starace, Phys. Rev. A **16**, 231 (1977).
[6] U. Becker, D. Szostak, M. Kupsch, H. G. Kerkhoff, B. Langer, and R. Wehlitz, J. Phys. B **22**, 749 (1989).
[7] Y. Azuma, S. Hasegawa, F. Koike, G. Kutluk, T. Nagata, E. Shigemasa, A. Yagishita, and I. A. Sellin, Phys. Rev. Lett. **74**, 3768 (1995).
[8] L. Journel, B. Rouvellou, D. Cubaynes, J.-M. Bizau, F. J. Wuilleumier, M. Richter, P. Sladeczek, K.-H. Selbmann, P. Zimmermann, and H. Bergeron, J. Phys. IV **3**, C6-217 (1993).
[9] S. Diehl *et al.*, Phys. Rev. Lett. **79**, 1241 (1997).
[10] S. Svensson, N. Mårtensson, and U. Gelius, Phys. Rev. Lett. **58**, 2639 (1987).
[11] J. E. Hansen, J. Phys. B **8**, L403 (1975).
[12] L. M. Kiernan, E. T. Kennedy, J.-P. Mosnier, J. T. Costello, and B. F. Sonntag, Phys. Rev. Lett. **72**, 2359 (1994).
[13] L. M. Kiernan, M.-K. Lee, B. F. Sonntag, P. Sladeczek, P. Zimmermann, E. T. Kennedy, J.-P. Mosnier, and J. T. Costello, J. Phys. B **28**, L161 (1995).
[14] L. Journel, D. Cubaynes, J.-M. Bizau, A. Moussalami, B. Rouvellou, F. Wuilleumier, L. VoKy, P. Faucher, and A. Hibbert, Phys. Rev. Lett. **76**, 30 (1996).
[15] S. Diehl *et al.*, Phys. Rev. Lett. **76**, 3915 (1996).
[16] R. Wehlitz, M.-T. Huang, B. D. DePaola, J. C. Levin, I. A. Sellin, T. Nagata, J. W. Cooper, and Y. Azuma, Phys. Rev. Lett. **81**, 1813 (1998).
[17] E. Shigemasa, Y. Yan, and A. Yagishita, KEK Report No. 95-2, 1995 (unpublished).
[18] Y. Sato *et al.*, J. Phys. B **18**, 225 (1985).
[19] Far ultraviolet photodiode; manufacturer, NIST, Serial No. 365.
[20] G. Mehlman, J. W. Cooper, and E. B. Saloman, Phys. Rev. A **25**, 2113 (1982).
[21] K. T. Chung and B.-C. Gou, Phys. Rev. A **52**, 3669 (1995).
[22] M.-T. Huang, R. Wehlitz, Y. Azuma, L. Pibida, I. A. Sellin, M. Koide, H. Ishijima, and T. Nagata, Phys. Rev. A **59**, 3397 (1999).
[23] U. Fano and J. W. Cooper, Phys. Rev. **137**, A1364 (1965).
[24] K. Berrington and S. Nakazaki, J. Phys. B **31**, 313 (1998).
[25] K. A. Berrington, W. Eissner, and P. N. Norrington, Comput. Phys. Commun. **92**, 290 (1995).
[26] L. Quigley and K. A. Berrington, J. Phys. B **29**, 4529 (1996).